forests

MDPI

Article

Exploring a New O_3 Index as a Proxy for the Avoidance/Tolerance Capacity of Forest Species to Tolerate O_3 Injury

Jacopo Manzini [1,2], Yasutomo Hoshika [1,3,*], Barbara Baesso Moura [1,4] and Elena Paoletti [1,3]

[1] Institute of Research on Terrestrial Ecosystems (IRET), National Research Council of Italy (CNR), Via Madonna del Piano 10, 50019 Sesto Fiorentino, Italy
[2] DAGRI, Department of Agriculture, Food, Environment and Forestry, University of Florence, Piazzale delle Cascine, 18, 50144 Firenze, Italy
[3] ITINERIS, Italian Integrated Environmental Research Infrastructures Systems, Tito Scalo, 85050 Potenza, Italy
[4] NBFC, National Biodiversity Future Center, 90133 Palermo, Italy
* Correspondence: yasutomo.hoshika@cnr.it

Abstract: Tropospheric ozone (O_3) is a detrimental air pollutant causing phytotoxic effects. Several O_3 indices are used to assess the risk for vegetation, e.g., the exposure-based AOT40 (accumulated ozone exposure over a threshold of 40 ppb) and the stomatal-flux based POD_1 (Phytotoxic Ozone Dose above a threshold of 1 nmol m^{-2} s^{-1}). Leaf Mass per Area (LMA) is recommended as a simple index to explain the plant tolerance capacity to O_3. We therefore tested a new species-specific O_3 index (Leaf Index Flux—LIF: calculated as stomatal O_3 flux/LMA) as a proxy of the avoidance/tolerance capacity against O_3 stress according to datasets of visible foliar injury (VFI) in forest monitoring and a manipulative Free-Air Controlled Exposure (FACE) experiment. For the forest monitoring, AOT40, POD_1, and LIF were calculated from hourly O_3, soil moisture, and meteorological measurements at nine Italian forest sites over the period 2018–2022. The results were tested for correlation with the O_3 VFI annually surveyed at the same sites along the forest edge (LESS) or inside the forest (ITP) and expressed as relative frequency of symptomatic species in the LESS (SS_LESS) and Plant Injury Index per tree in the plot (PII_ITP). Based on VFI occurrence at ITP and LESS, *Fagus sylvatica* was considered the most O_3-sensitive species, whereas conifers (*Pinus pinea* and *Picea abies*) and other deciduous/evergreen broadleaf (*Quercus petraea*, *Q. cerris*, *Q. ilex*, and *Phyllirea latifolia*) showed rare and no O_3 VFI. Shrub species such as *Rubus* spp. and *Vaccinium myrtillus* were O_3-sensitive, as they showed VFI along the LESS. AOT40 did not show significant correlations with the VFI parameters, POD_1 increased with increasing SS_LESS ($p = 0.005$, r = 0.37) and PII_ITP ($p < 0.001$, r = 0.53), and LIF showed an even higher correlation with SS%_LESS ($p < 0.001$, r = 0.63) and PII_ITP ($p < 0.001$, r = 0.87). In the FACE experiment, PII was investigated for five deciduous and three evergreen tree species following one growing season of exposure to ambient and above-ambient O_3 levels (PII_FACE). Moreover, PII_FACE resulted better correlated with LIF (r = 0.67, $p < 0.001$) than with POD_1 (r = 0.58, $p = 0.003$) and AOT40 (r = 0.35, $p = 0.09$). Therefore, LIF is recommended as a promising index for evaluating O_3 VFI on forest woody species and stresses high O_3 risk potential for forest species with high stomatal conductance and thin leaves.

Keywords: air pollution; flux-based index; ground-level O_3; POD_y; visible foliar injury

Citation: Manzini, J.; Hoshika, Y.; Moura, B.B.; Paoletti, E. Exploring a New O_3 Index as a Proxy for the Avoidance/Tolerance Capacity of Forest Species to Tolerate O_3 Injury. *Forests* **2023**, *14*, 901. https://doi.org/10.3390/f14050901

Academic Editor: Thomas Dirnböck

Received: 31 March 2023
Revised: 14 April 2023
Accepted: 21 April 2023
Published: 27 April 2023

1. Introduction

Ground-level ozone (O_3) is a secondary air pollutant arising from the interaction among solar radiation, high temperature, and its precursors (CH_4, NO_x, CO, and Volatile Organic Compounds) emitted by natural and anthropogenic sources [1,2]. Although a decrease in precursors' emissions led to a reduction of O_3 mean concentrations in North America, Europe, and Asia [3,4], an increase linked with high temperature is predicted in

the near future due to climate change [5], reaching 50–55 ppb in Europe by the end of the 21st century [6,7]. In particular, Southern European countries are among the most affected areas due to the local climatic conditions, such as a hot and dry summer, that favor O_3 photochemical formation in the troposphere [8].

Ozone is a significant abiotic stressor for plants, affecting their health and vitality [9]. Furthermore, as O_3 concentrations tend to be higher in rural and semi-rural areas than in cities [10], forests are highly threatened, and their essential ecosystem services, such as carbon sequestration [11] and biodiversity preservation [12], might be affected.

Ozone is absorbed by trees through stomata and stimulates the formation of Reactive Oxygen Species (ROS) [13]. Its phytotoxicity promotes the decline of photosynthesis and the alteration of stomatal physiology [14,15], leading to a reduction in growth [16] and productivity [17,18]. Furthermore, specific O_3-visible foliar injuries (O_3 VFI), such as typical chlorosis, black spots, and interveinal necrosis, due to the oxidation of leaf tissues [19–22], have been detected in various tree species across forest sites and can be used as a biological indicator to assess O_3 impacts on vegetation in the field [23]. Moreover, O_3 monitoring in forests is crucial, and several indices were developed to probe forest responses to this pollutant. Currently, the European directive for forest protection from O_3 (EU Directive 2008/50/EC) [24] is based on AOT40 (accumulated ozone exposure over a threshold of 40 ppb), an exposure-based index that accumulates the hourly concentrations of O_3 exceeding the threshold of 40 ppb over daylight hours during the growing season. However, the damages caused by O_3 are mainly related to its stomatal flux rather than its atmospheric concentration [25]. Hence, the National Emission Ceilings (NEC) Directive, within the framework of the Convention on Long-range Transboundary Air Pollution (CLRTAP), recently decided to include the Phytotoxic Ozone Dose (POD_Y) to assess O_3 impact on plant ecosystems [26]. POD_Y is a flux-based index that estimates stomatal O_3 uptake during the growing season above a threshold Y of potential phytotoxicity [22] and considers species-specific stomatal conductance responses to environmental conditions.

Nevertheless, other foliar structural traits beyond stomatal conductance, such as leaf morphology, may play a prominent role in O_3 sensitivity [20]. In particular, species with thick and dense leaves, such as Mediterranean evergreens, are stated to be more resistant to biotic and abiotic stressors [27]. Feng et al. [28] suggested that Leaf Mass per Area (LMA) could explain O_3 sensitivity variation among plant species. In fact, thick leaves have a relatively low mesophyll surface area exposed to O_3 [29] and cellular defense substrates per unit of stomatal O_3 flux increase with increasing LMA, as reported in spruce, pine, and larch trees [30].

Therefore, in the present study, we proposed a simple index called Leaf Index Flux (LIF) to weigh stomatal O_3 flux by LMA and correlate with O_3 VFI better than POD_1 or AOT40.

To provide realistic evidence and a proper species-specific examination, VFI was assessed both in the field, i.e., along Light Exposed Sampling Sites (LESS) of the forest edge or inside the forest plots (ITP), and in an O_3 Free-Air Controlled Exposure (FACE) facility.

Our aim was to verify whether LIF was well correlated with O_3 VFI under field and semi-controlled conditions and thus can be used as a proxy to assess O_3 VFI in forests. In addition, we tested which forest species were more O_3-sensitive when evaluated by applying LIF.

2. Materials and Methods

2.1. Forest Monitoring Network

The evaluation occurred from 2018 to 2022 in nine Italian forest sites belonging to a European monitoring network (MOTTLES—*MOnitoring ozone injury for seTTing new critical LevelS*) (Table 1). The sites covered distinct geographical areas of Italy and represent the Alpine, Continental, and Mediterranean biomes. The dominant forest species were conifers (*Pinus pinea* L. and *Picea abies* L.), deciduous broadleaf trees (*Fagus sylvatica* L., *Quercus*

petraea (Matt.) Liebl., and *Q. cerris* L.), and evergreen broadleaf trees (*Q. ilex* L. and *Phyllirea latifolia* L.).

Table 1. Features of the nine Italian sites belonging to the MOTTLES network.

Site Code	Geographic Coordinates	Altitude	Dominant Tree Species	Biome
ABR1	41.86064 N–13.57482 E	1500	*Fagus sylvatica*	Alpine
CPZ1	41.70423 N–12.35719 E	0	*Quercus ilex*	Mediterranean
CPZ2	41.70429 N–12.35732 E	0	*Phyllirea latifolia*	Mediterranean
CPZ3	41.68068 N–12.39084 E	0	*Pinus pinea*	Mediterranean
EMI1	44.71998 N–10.20345 E	200	*Quercus petraea*	Continental
LAZ1	42.82746 N–11.89817 E	690	*Quercus cerris*	Mediterranean
PIE1	45.68374 N–8.06994 E	1150	*Fagus sylvatica*	Alpine
TRE1	46.35825 N–11.49405 E	1800	*Picea abies*	Alpine
VEN1	46.06335 N–12.38810 E	1100	*Fagus sylvatica*	Alpine

The ozone concentrations and meteorological parameters were monitored at field stations powered by photovoltaic panels and placed in open fields (OFD) near the forest cover in each site [25]. In detail, O_3 concentrations were measured in real time by an active monitor (Model 106–L, 2B Technologies, Inc., Boulder, CO, USA), while the environmental variables recorded by specific sensors (DeltaOHM, Selvazzano Dentro, Italy) were air temperature (T), relative humidity (RH), solar radiation (photosynthetic active radiation: PAR), precipitation (rainfall), wind direction, and speed. Each sensor was installed 2 m above the ground. Hourly average data were recorded and transmitted remotely via GPRS connection. In case of signal absence, data were stored in data loggers (Campbell Scientific, Logan, UT, USA; Loughborough, UK) and subsequently downloaded manually. Maintenance and calibration were periodically performed every year. The soil water content (SWC) was measured within the forest plots (ITP), using sensors (Campbell Scientific, Logan, UT, USA; Loughborough, UK) randomly placed at a depth of 10 cm.

2.2. Ozone FACE Facility

A new-generation tridimensional O_3 FACE facility located in Sesto Fiorentino (43°48′59″ N, 11°12′01″ E, 55 m a.s.l.) was used to artificially fumigate potted plants by O_3. Further details about the facility are reported in Paoletti et al. [31]. Three evergreen (*Arbutus unedo* L., *Phillyrea angustifolia* L., and *Pinus pinea* L.) and five deciduous species (*Sorbus aucuparia* L., *Alnus glutinosa* (L.) Gaertn., *Vaccinium myrtillus* L., *Populus maximowiczii* Henry *X P.* × *berolinensis* Dippel, and *Populus x euramericana* I-214) were exposed to three O_3 levels (Ambient Air, 1.5 × Ambient Air, and 2.0 × Ambient Air) during the growing season and well-watered every day to maintain field capacity. Hourly average data related to environmental parameters (T, RH, PAR, and wind) were recorded during the experimental period of each year by a Watchdog station (Mod. 2000; Spectrum Technology, Inc., Aurora, IL, USA) placed at 2.5 m above ground level.

2.3. Calculation of O_3 Indices: AOT40, POD_1 and LIF

The accumulated ozone exposure over a threshold of 40 ppb (AOT40; ppb h) was calculated by summing all hourly average O_3 concentrations exceeding the threshold of 40 ppb during daylight hours (shortwave solar radiation > 50 W m^{-2}) from the beginning of the growing season to the time of the VFI survey, according to the following formula:

$$\text{AOT40 (ppb·h)} = \sum_{i=1}^{n} max([O_3]i - 40,\ 0) \cdot \Delta t$$

This index assumes that vegetation does not suffer damage with O_3 concentrations lower than 40 ppb (AOT40 = 0) and that, during the night, the stomata are closed and

prevent the entry of O_3. The critical level for forest protection based on accumulated ozone exposure over a threshold of 40 ppb (AOT40) is 5000 ppb h, corresponding to a 5% reduction in tree biomass [32] (CLRTAP, 2017).

Regarding the Phytotoxic Ozone Dose (POD_Y), the following formula was used to carry out the calculation:

$$POD_Y \left(\text{mmol m}^{-2}\right) = \sum_{i=1}^{n} (F_{st,i} - Y) \cdot \Delta t$$

where F_{st} represents the hourly stomatal O_3 flux, n is the number of hours for the period considered, and Δt = 1 h. We considered a Y threshold of 1 nmol O_3 m^{-2} s^{-1} (POD_1), as suggested by the UNECE Mapping Manual of CLRTAP [32].

Finally, the Leaf Index Flux (LIF) was calculated as the ratio between species-specific POD_1 and Leaf Mass per Area (LMA) and was expressed in mmol O_3 g^{-1}:

$$\text{Leaf Index Flux (LIF)} = \frac{\text{POD1}}{\text{LMA}}$$

The Leaf Index Flux was calculated ex novo for the forest sites (LESS and ITP) and by using published data [33] for the species subjected to artificial fumigation with O_3 in the FACE facility.

2.4. Stomatal O_3 Flux Modelling

The hourly stomatal O_3 flux F_{st} (nmol m^{-2} s^{-1}), considered in the POD_1 calculation, was obtained as follows:

$$F_{st} = [O_3] \cdot \left\{ \frac{1}{R_b + R_c} \right\} \cdot \left\{ \frac{g_{sto}}{g_{sto} + g_{ext}} \right\}$$

where $[O_3]$ is the hourly O_3 concentration (ppb), R_b is the boundary layer resistance (s m^{-1}), R_c is the leaf surface resistance (s m^{-1}), g_{sto} is the stomatal conductance (mmol O_3 m^{-2} s^{-1}), and g_{ext} is the cuticular conductance (m s^{-1}). In detail, $R_b = 1.3 \times 150 \times (L_d/u)^{0.5}$, where L_d is the leaf size; and u is the wind speed, expressed in m s^{-1}.

The stomatal conductance (g_{sto}) estimation was based on the multiplicative model described by Jarvis [34] and modified by CLRTAP [32] according to the following equation [15]:

$$g_{sto} = g_{max} \times f_{phen} \times f_{light} \times max\{f_{min}, (f_{temp} \times f_{VPD} \times f_{SWC})\}$$

where g_{max} represents the maximum stomatal conductance, while f_{phen}, f_{light}, f_{temp}, f_{VPD}, and f_{swc} are functions that indicate the variation of g_{sto} in relation to phenology, photosynthetic active radiation (PAR, µmol m^{-2} s^{-1}), air temperature (T, °C), vapor pressure deficit (VPD, kPa) and soil moisture (SWC, m^3 m^{-3}), respectively. Finally, f_{min} represents the minimum stomatal conductance. The functions used are detailed below.

$$f_{light} = 1 - \exp(-\text{light}_a \cdot \text{PAR})$$

where $light_a$ is a dimensionless coefficient for curvature of stomatal conductance response to PAR.

$$f_{temp} = \left(\frac{T - T_{min}}{T_{opt} - T_{min}} \right) \left\{ \left(\frac{T_{max} - T}{T_{max} - T_{opt}} \right)^{\left(\frac{T_{max} - T_{opt}}{T_{opt} - T_{min}} \right)} \right\}$$

where T_{max}, T_{min}, and T_{opt} are the maximum, minimum, and optimal temperatures for the stomata opening, respectively.

$$f_{VPD} = \min\left[1, \max\left\{f_{min}, \left(\frac{(1 - f_{min}) \cdot (VPD_{min} - VPD)}{(VPD_{min} - VPD_{max})} \right) + f_{min} \right\}\right]$$

where VPD_{min} and VPD_{max} are, respectively, the vapor pressure deficit to reach the minimum and maximum stomatal opening.

$$f_{SWC} = \min\left[1,\ \max\left\{f_{min}, (1 - f_{min})\left(\frac{SWC - WP}{FC - WP}\right) + f_{min}\right\}\right]$$

where SWC is soil moisture, WP is the wilting point, and FC is the field capacity obtained from Anav et al. [35]. Finally, f_{phen} was set equal to 1 during the growing season. The start of the growing season was based on a phenological model in the forest [25] and by direct observations in the FACE experiment. The end of the accumulation window was the time of the VFI survey.

We applied the species-specific stomatal conductance model parameters in the target species reported in our previous papers [15,23,36] and the CLRTAP mapping manual [32]. The applied parameters are listed in Supplementary Table S1.

2.5. Calculation of Leaf Mass per Area (LMA)

To assess the species-specific LMA, five leaf discs of 0.8 cm in diameter were obtained by a leaf punch (Fujiwara Scientific Company Co., Ltd., Tokyo, Japan) for each sampled light-exposed leaf (n = 5 leaves × 3 plants per site for MOTTLES sites, for 3 leaves × 1 to 2 plants per plot × 3 replicated plots × 2 to 3 O_3 levels for the FACE experiments). The leaf discs were oven-dried at 70 °C for 72 h and weighed by an analytical balance (Sartorius, Goettingen, Germany). The projected needle area of the samples was assessed by Easy Leaf Area application [37]. The LMA, expressed in g m^{-2}, was finally calculated as the ratio between dry biomass and area.

2.6. Surveys of O_3 Visible Foliar Injury

As suggested by the *ICP Forests Manual* for O_3 injury assessment [38], in the MOTTLES sites, O_3 VFI was determined along the LESS and inside the forest (ITP), i.e., at around 600 m from the OFD. Every year, at the end of the growing season, a team of two expert evaluators carried out an estimate of O_3 VFI (interveinal black/reddish necrosis in the upper leaf surfaces, [38]) at each LESS and ITP forest site (Supplementary Figure S1). The evaluation was performed on current-year light-exposed leaves/needles. The ozone VFIs were validated for each species based either on the literature or on one-year exposure in the O_3 FACE facility [23]. Concerning LESS, a forest edge of 50 m in length and 1 m in depth was examined. The area was divided into 25 adjacent and non-overlapping quadrates of 2 m^2 each, randomly excluding 5 quadrates, as Schaub et al. [38] suggested. The plant species were cataloged in each quadrate, and the presence/absence of O_3 VFI was recorded. For each species in the LESS, the following relative frequency of symptomatic species was calculated:

$$SS\_LESS = \frac{\text{number of LESS quadrates with symptomatic species}}{\text{total number of LESS quadrates where the target species is present}} \times 100$$

Within each ITP, sampling was performed on five randomly selected trees belonging to the dominant species. Depending on the species, 5 branches exposed to the light, with at least 30 leaves or needles, were evaluated. The Plant Injury Index (PII) was obtained by combining the percentage of injured leaves per shoot (LA) and the percentage of injured leaf surface per symptomatic leaf (AA), as suggested by Paoletti et al. [39]. Finally, an average was made for the five branches, thus obtaining an average percentage value of O_3 VFI per tree (PII_ITP).

$$PII\_ITP = \frac{LA \times AA}{100}$$

The Plant Injury Index was assessed in light-exposed leaves that were grown during the season, as well as for the plants in the O_3 FACE facility (PII_FACE) in September,

except for *Alnus glutinosa* and *Vaccinium myrtillus*, for which the PII was assessed in July (Supplementary Figure S1).

2.7. Statistical Analyses

For the MOTTLES datasets, only forest sites with at least 75% validated data of hourly environmental parameters and O_3 concentrations were considered. POD_1, AOT40, and LIF were related to SS_LESS and PII_ITP for each site, or to PII_FACE for the FACE facility. Normal distribution was tested with the Lilliefors test (Kolmogorov–Smirnov). The significance ($p < 0.05$) of the linear regression lines was verified using the Pearson's correlation coefficient (r). Moreover, we performed a one-way ANOVA to assess if O_3 significantly affected species-specific LMA values during the FACE experiment. Statistical analyses were conducted with MS Excel (Microsoft ®).

3. Results

3.1. Meteorological Conditions and Ozone Concentrations

3.1.1. MOTTLES Sites

The highest daily mean O_3 concentration was detected in Abruzzo (ABR1) and was equal to 52.13 ppb during the period considered (2018–2022, Table 2). The lowest values were recorded in Castelporziano (CPZ1, CPZ2, and CPZ3), corresponding to 29.58 ppb. The highest average daily mean temperature (16.30 °C) was recorded in Castelporziano, while the lowest was in TRE1 (5.25 °C). Moreover, the daily mean photosynthetically active radiation was higher in Castelporziano (412.73 μmol m^{-2} s^{-1}), but the lower value was at PIE1 (305.80 μmol m^{-2} s^{-1}). The relative humidity and soil water content showed the highest values at VEN1 (86.80% and 40.38%, respectively), while the lowest values of VPD were found at VEN1 (0.17 kPa), followed by TRE1 (0.29 kPa), PIE1 (0.31 kPa) and ABR1 (0.31 kPa). Finally, the wettest sites were PIE1 and VEN1, with an average of more than 1700 mm of annual rainfall.

Table 2. Recorded annual averages of air temperature (T), relative humidity (RH), vapor pressure deficit (VPD), photosynthetically active radiation (PAR), soil water content at 10 cm depth (SWC), annual rainfall and daily O_3 concentration at the 9 Italian forest sites. Data refer to the period 2018–2022 ± standard error.

Site	T (°C)	RH (%)	VPD (kPa)	PAR (μmol m^{-2} s^{-1})	SWC (%)	Rainfall (mm)	O_3 (ppb)
ABR1	7.67 ± 0.27	75.90 ± 2.00	0.31 ± 0.04	374.44 ± 10.67	28.90 ± 1.30	893.81 ± 157.73	52.13 ± 2.08
CPZ *	16.30 ± 0.25	78.60 ± 1.00	0.47 ± 0.04	412.73 ± 14.63	13.01 ± 0.84	623.95 ± 125.79	29.58 ± 2.16
EMI1	13.11 ± 1.11	74.00 ± 1.00	0.51 ± 0.09	314.36 ± 14.75	15.06 ± 0.65	793.43 ± 101.91	36.50 ± 2.14
LAZ1	13.54 ± 0.25	73.50 ± 2.00	0.52 ± 0.06	369.75 ± 11.64	17.38 ± 0.71	1304.82 ± 328.57	45.59 ± 1.53
PIE1	8.52 ± 0.96	74.20 ± 1.00	0.31 ± 0.02	305.80 ± 11.38	27.31 ± 1.79	1765.56 ± 363.59	50.20 ± 1.09
TRE1	5.25 ± 0.55	70.50 ± 1.00	0.29 ± 0.03	361.84 ± 21.82	39.45 ± 4.41	814.65 ± 113.49	45.61 ± 2.45
VEN1	7.56 ± 0.39	86.80 ± 1.00	0.17 ± 0.02	329.30 ± 13.79	40.38 ± 0.43	1703.58 ± 291.60	33.96 ± 0.94

* Data are the same for CPZ1, CPZ2, and CPZ3, except for SWC, as it is equal to 16.72 ± 1.83 in CPZ3.

3.1.2. FACE Experiments

Table 3 shows the daily means of meteorological data and O_3 concentrations in the FACE experiments. The highest temperature and VPD were recorded in 2017 (24.50 °C and 1.89 kPa, respectively), while the lowest ones occurred in 2020 (22.10 °C and 1.31 kPa, respectively). The relative humidity showed the highest value in 2020 (61.80%) and the lowest one in 2017 (47.60%). The photosynthetically active radiation was always higher than 500 μmol m^{-2} s^{-1} (maximum value 578 μmol m^{-2} s^{-1} in 2016), except in 2020 (PAR = 475 μmol m^{-2} s^{-1}). Regarding O_3, the Ambient Air concentration was in a range of 35–40 ppb for the reference years (2016–2020).

Table 3. Recorded daily mean ± standard error of air temperature (T), relative humidity (RH), vapor pressure deficit (VPD), photosynthetically active radiation (PAR), and daily O_3 concentration at FACE experiment for years 2016–2020. Plants were subjected to three levels of O_3 (AA—Ambient Air, 1.5 × Ambient Air, and 2.0 × Ambient Air).

Year	T (°C)	RH (%)	VPD (kPa)	PAR (μmol m^{-2} s^{-1})	O_3 (ppb)		
					AA	1.5×	2.0×
2016	22.90 ± 0.30	57.00 ± 3.00	1.50 ± 0.08	578 ± 13	34.7 ± 0.60	51.2 ± 0.90	66.1 ±1.00
2017	24.50 ± 0.40	47.60 ± 1.30	1.89 ± 0.08	564 ± 16	40.3 ± 1.20	51.7 ± 1.80	63.8 ± 2.30
2018	22.80 ± 0.29	55.60 ± 0.83	1.48 ± 0.04	527 ± 13	35.2 ± 0.70	53.1 ± 1.10	65.2 ± 1.40
2019	23.50 ± 0.35	55.10 ± 0.94	1.61 ± 0.06	548 ± 14	38.8 ± 0.90	56.2 ± 1.50	68.6 ± 1.80
2020	22.10 ± 0.39	61.80 ± 1.12	1.31 ± 0.05	475 ± 17	37.5 ± 1.10	52.3 ± 1.70	73.3 ± 2.30

3.2. Leaf Mass per Area

3.2.1. MOTTLES Sites

The highest LMA values were found for the conifers *Picea abies* (262.10 g m^{-2}) and *Pinus pinea* (192.47 g m^{-2}; Supplementary Table S2). Among the deciduous trees, *Fagus sylvatica* showed the lowest values (between 50.42 and 67.01 g m^{-2}), while the evergreens *Quercus ilex* (142.65 g m^{-2}) and *Phillyrea latifolia* (144.64 g m^{-2}) showed the highest values. For LESS species, *Rubus* spp. and *Vaccinium myrtillus* LMA ranged from 55 to 78 and from 35 to 56 g m^{-2}, respectively.

3.2.2. FACE Experiments

As confirmed in the MOTTLES sites, evergreen species showed a relatively high LMA value relative to deciduous species (Supplementary Table S3). The lowest LMA values were found in a fast-growing deciduous species, *Alnus glutinosa* (approximately 48 g m^{-2}). For most of the species, O_3 did not significantly affect LMA values, except for Oxford poplar clone (*Populus maximowiczii* Henry × *P. berolinensis* Dippel) in 2016 (one-way ANOVA, $p = 0.047$) and *Phillyrea angustifolia* in 2018 (one-way ANOVA, $p = 0.025$).

3.3. Ozone Visible Foliar Injury at LESS, ITP and FACE

At the MOTTLES sites, *Fagus sylvatica* showed O_3 VFI within the LESS during all the years at VEN1, PIE1, and ABR1 (Table 4). Within all the LESS quadrates, O_3 VFI was found in *F. sylvatica* leaves at PIE1 in both 2020 and 2021, and at VEN1 in 2022 (SS_LESS = 100%). High frequencies for this species (70–90%) were also found at VEN1 in 2019, 2020, and 2021, while the lowest percentages (20–47%) were recorded at ABR1. Concerning *Rubus* spp., SS_LESS = 100% was quantified at CPZ3 during 2020. On the contrary, for 2021 and 2022, no plants of *Rubus* spp. showed O_3 VFI at CPZ3 (SS_LESS = 0%). Injured *Rubus* plants were also found at LAZ1, PIE1, and EMI1 with SS_LESS equal to 64.2 and 66.6% in 2022 for the latter two sites, respectively. Injured *Vaccinium myrtillus* was observed in the LESS of PIE1 (in 2018, 2021, and 2022) and TRE1 (period 2019-2022). In particular, SS%_LESS increased from 2019 to 2022 at TRE1, passing from 44 to 100%, while O_3 VFI was found at PIE1 (66.6%) only in 2022. No dominant species in the LESS (*P. pinea*, *P. abies*, *Q. petraea*, *Q. cerris*, and *P. latifolia*) showed O_3 VFI, except for *P. abies* (SS_LESS = 16.6%) in 2022, at TRE1. Regarding ITP, O_3 VFI was found only in *Fagus sylvatica*, *Pinus pinea*, and *Picea abies* (Table 5). The highest value of PII_ITP for *F. sylvatica* was 8.90% at VEN1 in 2020, while the lowest value (0.30%) was recorded at ABR1 in the same year. *Pinus pinea* showed an O_3 foliar injury at CPZ3 only in 2018, with a PII_ITP equal to 0.44%, while *Picea abies* at TRE1 showed a PII_ITP of 0.32%. The other dominant species, such as *Quercus petraea*, *Q. ilex*, *Q. cerris*, and *Phyllirea latifolia* did not show O_3 VFI during the ITP surveys in any year.

Table 4. Relative frequency of symptomatic species within the LESS (SS_LESS) for the period 2018–2022.

Year	LESS Site	*Fagus sylvatica*	*Rubus* spp.	*Vaccinium myrtillus*	*Picea abies*
2018	VEN1	55			
	ABR1	20			
	PIE1	56			
2019	VEN1	90			
	ABR1	45			
	PIE1	50			
	TRE1			44	
2020	VEN1	70			
	ABR1	25			
	PIE1	100			
	LAZ1		10		
	CPZ3		100		
	TRE1			63	
2021	VEN1	90			
	ABR1	47			
	PIE1	100	9		
	EMI1		20		
	LAZ1		57		
	TRE1			79	
2022	VEN1	100			
	ABR1	40			
	PIE1	40	64.2	66.6	
	EMI1		66.6		
	TRE1			100	16.6

Table 5. Average percentage value ± standard error of O_3 VFI per tree (PII_ITP) for each species inside the forest plot (ITP; $n = 5$).

Year	ITP Site	*Fagus sylvatica*	*Pinus pinea*	*Picea abies*
2018	VEN1	7.41 ± 2.15		
	ABR1	6.90 ± 3.08		
	PIE1	2.20 ± 0.91		
	CPZ3		0.44 ± 0.35	
2019	VEN1	6.40 ± 3.60		
	PIE1	1.50 ± 0.49		
2020	VEN1	8.90 ± 1.99		
	ABR1	0.30 ± 0.06		
	PIE1	3.98 ± 1.63		
2021	VEN1	4.90 ± 1.05		
	ABR1	1.48 ± 0.56		
	PIE1	0.41 ± 0.13		
	TRE1			0.32 ± 0.10
2022	VEN1	7.12 ± 1.50		
	ABR1	0.68 ± 0.29		
	PIE1	1.85 ± 0.80		

At the FACE, a relatively high PII was shown in deciduous species (Table 6). The PII increased with increasing O_3 levels. The highest PII was shown in *Sorbus aucuparia* exposed to 2.0 × Ambient Air O_3 treatment, which was more than 11%. On the other hand, evergreen species showed a very low PII (e.g., *P. pinea* and *P. angustifolia* showed PII_FACE = 0).

Table 6. Plant Injury Index (PII) for species subjected to fumigation in O_3 FACE (years 2016–2020). For each O_3 treatment (Ambient Air, 1.5×, and 2.0×), the species-specific PII (mean ± standard error) is shown.

Year	Species	O_3 Treatment	PII (%)
2016	*Populus maximowiczii* Henry *X P.* × *berolinensis* Dippel	Ambient Air	1.52 ± 0.74
		1.5×	5.79 ± 1.99
		2.0×	9.07 ± 1.96
2017	*Arbutus unedo*	Ambient Air	0.01 ± 0.01
		1.5×	0.01 ± 0.01
		2.0×	0.08 ± 0.05
2018	*Phillyrea angustifolia*	Ambient Air	0
		1.5×	0
		2.0×	0
2018	*Vaccinium myrtillus*	Ambient Air	1.76 ± 0.64
		2.0×	9.14 ± 0.35
2018	*Sorbus aucuparia*	Ambient Air	3.99 ± 0.71
		2.0×	11.27 ± 2.40
2018	*Alnus glutinosa*	Ambient Air	0.66 ± 0.51
		2.0×	7.04 ± 1.88
2019	*Pinus pinea*	Ambient Air	0
		1.5×	0
		2.0×	0
2020	*Populus maximowiczii* Henry *X P.* × *berolinensis* Dippel	Ambient Air	1.52 ± 0.79
		1.5×	6.29 ± 2.02
		2.0×	10.02 ± 2.11
2020	*Populus x euramericana* I-214	Ambient Air	0.09 ± 0.02
		1.5×	1.88 ± 0.72
		2.0×	4.02 ± 1.33

3.4. AOT40 and POD_1 versus Visible Foliar Injury

The AOT40 was higher at ABR1 than at the other sites for three out of the five years, with a maximum of 54,588 ppb·h recorded in 2018 (Supplementary Table S4 and Figure 1). The lowest values were at TRE1 (2019–2021) and CPZ (2018 and 2022), with a minimum of 8377 ppb·h at CPZ in 2022. POD_1 did not depend on site conditions or on the species. For *F. sylvatica*, the highest POD_1 values were at VEN1 (30.88 mmol m^{-2} in 2018), and the lowest ones were at ABR1 (6.43 mmol m^{-2}). High POD_1 values for this species at VEN1 were associated to the highest PII_ITP among all sites and years.

Concerning *Rubus* spp., the highest POD_1 (14.69 mmol m^{-2}) and 100% SS_LESS were at CPZ3 in 2020. For *V. myrtillus*, POD_1 values were always high at TRE1 with a maximum of 28.47 mmol m^{-2} in 2021, where SS_LESS values were also high. Interestingly, *Picea abies* showed a relatively high POD_1 value at TRE1 (18.12–33.01 mmol m^{-2}). However, visible foliar injuries were rarely seen for this species, as confirmed by very low values of both SS_LESS and PII_ITP.

At the FACE, AOT40 values in Ambient Air conditions were 13,774 to 24,243 ppb·h (Supplementary Table S5) and increased with increasing enhanced O_3 levels. POD_1 values were species-specific, with a maximum in Oxford poplar clone (75.15 mmol m^{-2}) and a relatively low value (2.79–6.13 mmol m^{-2}) for the Mediterranean evergreen shrub *Arbutus unedo*.

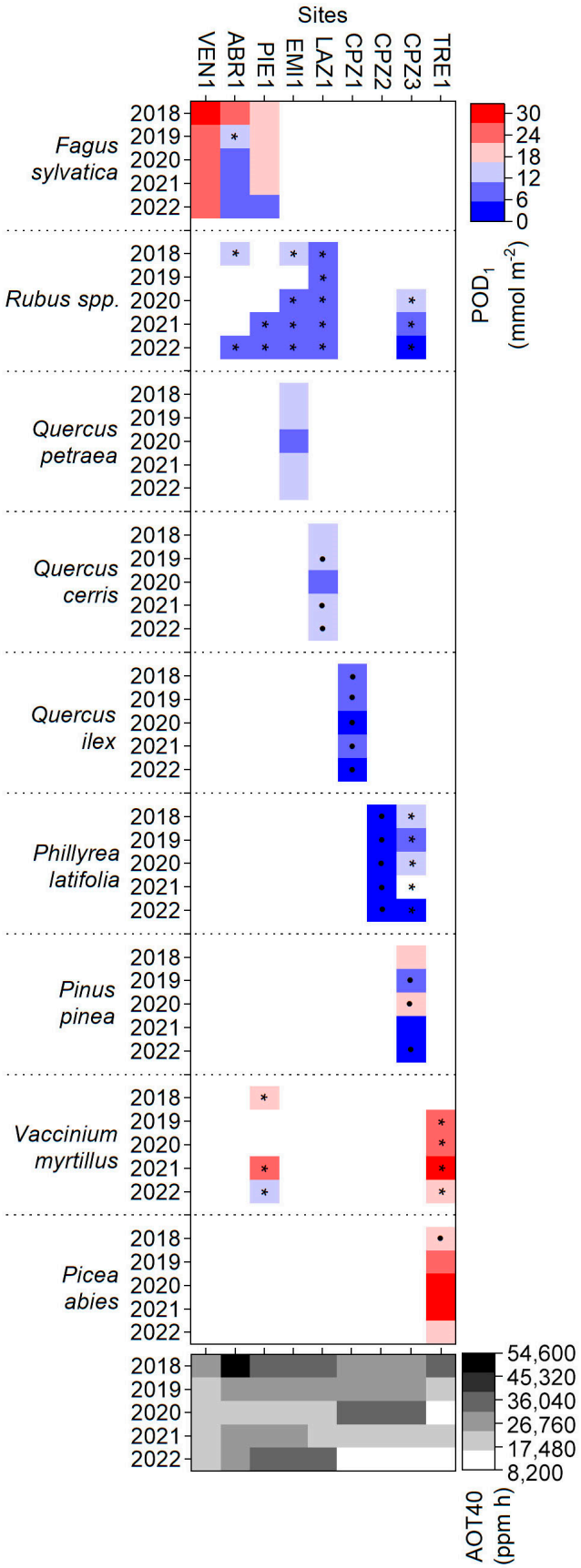

Figure 1. Annual values of AOT40 and POD_1 for each site. The symbols • and * refer to species present only in the ITP or LESS, respectively. If no symbols are present, species were found in both LESS and ITP.

The relationship between species-specific POD_1 calculated for LESS-species and their relative frequency of O_3 VFI (SS_LESS) was statistically significant (p = 0.005, r = 0.37; Figure 2A), while AOT40 and SS_LESS were not correlated (r = 0.11, p = 0.40). The percentage of ITP O_3 VFI (PII_ITP) increased with the POD_1 values calculated for all the dominant species at each site (r = 0.53, $p < 0.001$; Figure 2C), while AOT40 was not correlated with PII_ITP (r = 0.03, p = 0.85). Such a tendency was also confirmed in the FACE, where the correlation between PII_FACE and AOT40 was not significant, while it was for POD_1 (Figure 3A,B). Moreover, AOT40 did not correlate with POD_1 (r = 0.003, p = 0.97).

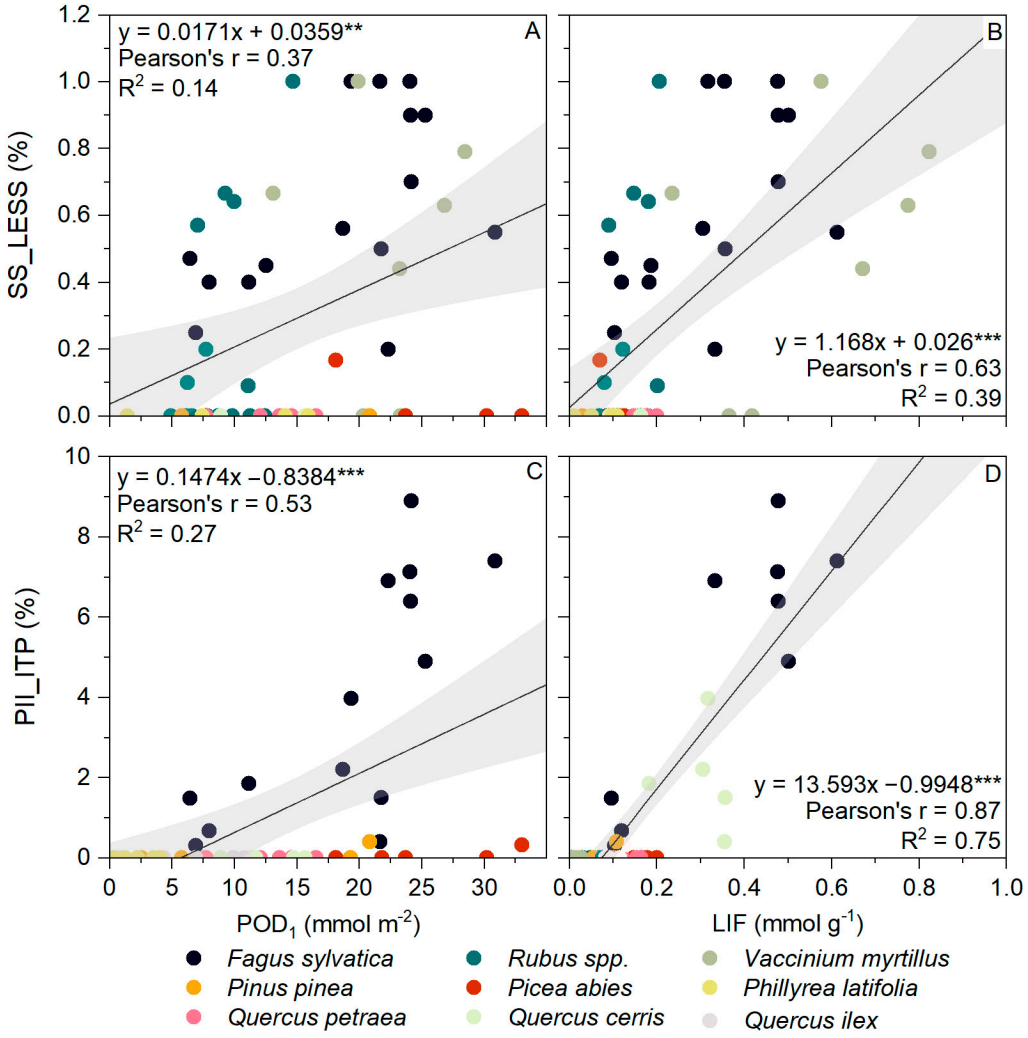

Figure 2. (**A**) Linear relationship (p = 0.005) between species-specific POD_1 and relative frequency of O_3 VFI (SS_LESS) over the period 2018–2022 (n = 55). (**B**) Linear relationship ($p < 0.001$) between LIF and relative frequency of O_3 VFI (SS_LESS) over the period 2018–2022 (n = 55). (**C**) Linear relationship ($p < 0.001$) between species-specific POD_1 and mean percentage value of leaf area affected by O_3 VFI for ITP-dominant species (PII_ITP) over the period 2018–2022 (n = 44). (**D**) Linear relationship ($p < 0.001$) between LIF and mean percentage value of leaf area affected by O_3 VFI for ITP-dominant species (PII_ITP) over the period 2018–2022 (n = 44). The linear regression lines show 95% confidence intervals in gray. ** $p < 0.01$, *** $p < 0.001$.

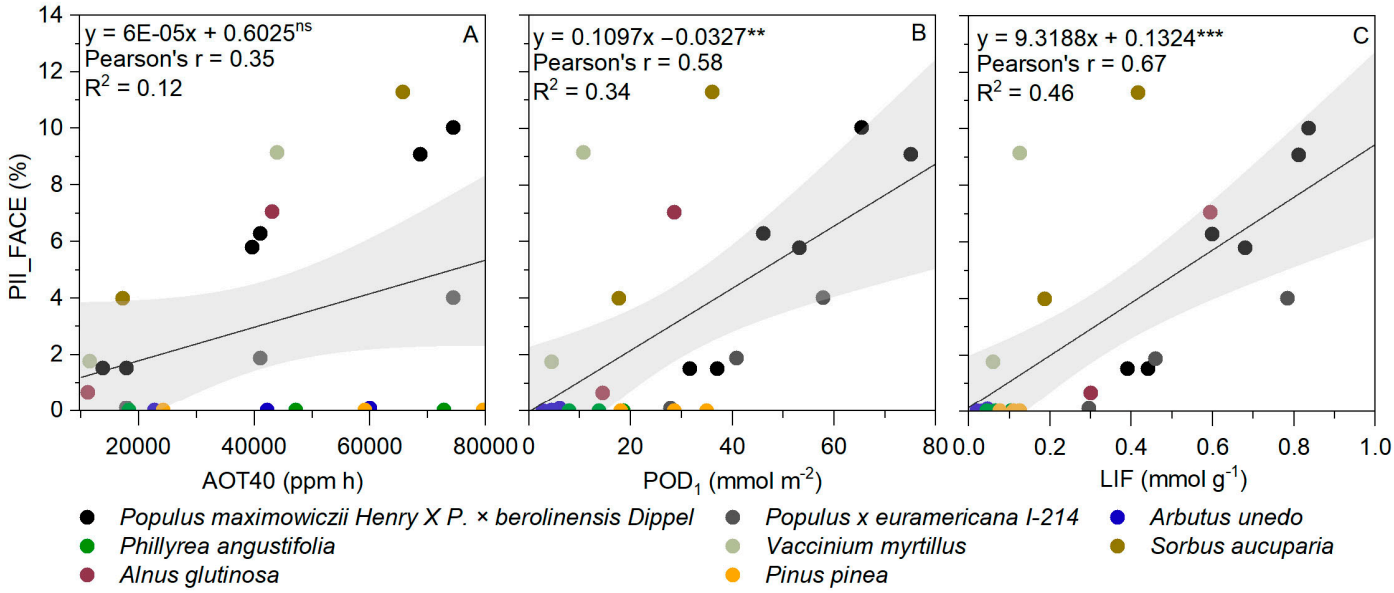

Figure 3. (**A**) Linear relationship (p = 0.09, ns) between AOT40 and Plant Injury Index (PII_FACE) calculated for species hosted in the O_3 FACE (n = 25). (**B**) Linear relationship (p = 0.003) between POD_1 and Plant Injury Index (PII_FACE) calculated for species hosted in the O_3 FACE (n = 25). (**C**) Linear relationship ($p < 0.001$) between LIF and Plant Injury Index (PII_FACE) calculated for species hosted in the O_3 FACE (n = 25). The linear regression lines show 95% confidence intervals in gray. ns not significant, ** $p < 0.01$, *** $p < 0.001$.

3.5. LIF versus Visible Foliar Injury

The LIF was calculated for each species and was significantly correlated to SS_LESS (r = 0.63, $p < 0.001$; Figure 2B) and PII_ITP (r = 0.87, $p < 0.001$; Figure 2D). Moreover, a significant strong positive correlation (r = 0.70, $p < 0.001$) between POD_1 and LIF was detected. Conversely, AOT40 did not correlate with the LIF (r = 0.03, p = 0.74). Interestingly, the Plant Injury Index (PII_FACE) calculated at the end of growing season for species exposed to O_3 in the FACE facility confirmed that the LIF had a higher correlation (r = 0.67, $p < 0.001$; Figure 3C) with PII_FACE than with AOT40 (r = 0.35, p = 0.09; Figure 3A) and POD_1 (r = 0.58, p = 0.003; Figure 3B).

4. Discussion

4.1. Different Sensitivity to O_3 among Species according to Visible Foliar Injury

For the dominant tree species inside the forest plots considered in this study (ITP), *Fagus sylvatica* was the most sensitive species, as it showed O_3 VFI at three sites (ABR1, PIE1, and VEN1) in the period of 2018–2022. Our results are in agreement with those of previous studies carried out in nurseries [40], FACE facilities [41], and open-top chambers [42], denoting that beech is characterized by low O_3 tolerance and the early appearance of O_3 VFI, mainly identifiable as browning and dark spots. Conifers were better at tolerating the abiotic stress due to O_3. In fact, O_3 VFI was found only in 2018 at CPZ3 for *P. pinea* and in 2021 at TRE1 for *P. abies*. The high tolerance for *P. pinea* was confirmed in the FACE, where O_3 VFI was not observed even under twice the ambient O_3 levels. The dominant broadleaf species present in the other forest sites located in Central–Southern Italy, such as *Quercus ilex*, *Quercus cerris*, *Quercus petraea*, and *Phillyrea latifolia*, did not show any O_3 VFI. First of all, those representative species of the Mediterranean area evolved in an environment constantly subjected to other oxidative stresses, such as long dry periods and high solar irradiation, and are likely endowed with an efficient antioxidant pool for the detoxification of O_3 inside the leaf parenchyma [43]. Experiments carried out in open-top chambers [44] also reported that *Quercus ilex* plants were asymptomatic even after two years of exposure to high O_3 concentrations (approximately daily mean of 40 ppb). In

the LESS, *Fagus sylvatica* showed O_3 VFI, although young trees, usually present at forest edges, may be more sensitive to O_3 than adult ones [45] due to lower stomatal conductance of mature trees than juvenile trees caused by a greater resistance to height-dependent water transport [46,47]. In addition, shrub species (*Rubus* spp.) and underbrush plants (*Vaccinium myrtillus*) were symptomatic during LESS surveys. A relatively high sensitivity of *V. myrtillus* in terms of O_3 VFI was also confirmed in the FACE. A long-term exposure to high concentrations of O_3 also resulted in an alteration of the yield and nutraceutical quality of fruits, suggesting that *Vaccinium myrtillus* is sensitive to O_3 [48]. In addition to the above-mentioned species, according to the FACE experiments, *Sorbus aucuparia* and poplar species were considered to be O_3-sensitive, as they showed a high PII due to a high stomatal O_3 uptake.

4.2. Which Is the Best Index for Ozone Visible Foliar Injury

Concerning the O_3 indices investigated in this work, several studies suggest that AOT40 can provide misleading results if used as the only reference metric for forest protection from O_3 (e.g., Anav et al. [34]). Confirming this, although AOT40 values in our target sites were always much higher than the regulatory limit for the protection of forests set by CLRTAP [32] at 5000 ppb h, no significant correlation was found between AOT40 and O_3 VFI. On the contrary, POD_1 increased with the increase of both injury parameters, highlighting that a flux-based index is more appropriate than AOT40 for the definition of species-specific critical levels and the consequent protection of forests. Indeed, asymptomatic *Phillyrea latifolia* and *Quercus ilex* had relatively low POD_1 values in Castelporziano (CPZ1 and CPZ2); the values were lower than the critical level indicated by Sicard et al. [49] for hardwoods, i.e., 12 mmol m^{-2}, while *Fagus sylvatica* and *Vaccinium myrtillus* regularly exceeded this POD_1 critical level and showed VFI in Northern Italian sites (PIE1 and VEN1). Confirming this, the two poplar clones tested in the FACE experiment, i.e., *Populus maximowiczii Henry X P. × berolinensis Dippel* and *Populus x euramericana I-214*, characterized by very high stomatal conductance (g_{max} equal to 348 and 478 mmol O_3 m^{-2} PLA s^{-1}, respectively), exceeded the critical threshold of 12 mmol m^{-2} (POD_1 about 2–3 times higher in Ambient Air treatment), resulting in severe damage, as indicated by PII, while *Arbutus unedo* (g_{max} equal to 95 mmol O_3 m^{-2} PLA s^{-1}) exhibited low POD_1 and limited symptoms (PII = 0.01–0.08%). However, several species showed very few symptoms, although they had a relatively high value of POD_1 (18.12–33.01 mmol m^{-2} for *P. abies*, 7.73–16.51 mmol m^{-2} for *Q. petraea*, and 8.89–15.66 mmol m^{-2} for *Q. cerris* in the years considered) that was, on average, higher than the critical level of 5 and 12 mmol m^{-2} recommended for conifers and broadleaves, respectively [49]. This study thus developed and tested the LIF, an index that explores the sensitivity to O_3 of forest species as a function of not only stomatal flux as a proxy of avoidance capacity but also LMA, a representative parameter of the leaf morphology as a proxy of defense capacity against O_3. Interestingly, in forest-monitoring data, we found a strong significant correlation ($p < 0.001$) of O_3 VFI (SS_LESS and PII_ITP) with LIF, even higher than with POD_1. Moreover, we confirmed that LIF fitted better than the other two indices also in experimental conditions with O_3-fumigated plants in a manipulative FACE experiment. Plant resistance to oxidative stress due to O_3 exposure can be explained not only by avoidance (restriction of O_3 entry via stomata) but also by tolerance (biochemical defense and repair) [50]. Since LIF considered both avoidance and tolerance against O_3, it is proposed as an interesting and effective new proxy for evaluating O_3 damages on forest species. Species characterized by high LMA values (and consequent low LIF), such as *Picea abies*, *Pinus pinea*, and the Mediterranean sclerophyllous *Quercus ilex* and *Phyllirea latifolia* may cope well with the oxidative stress caused by O_3. Several studies reported that leaves characterized by high LMA values possess high antioxidant capacities [30,44,51]. In particular, Mediterranean sclerophyllous plants, which are often suffering from drought, high irradiance, and/or O_3, have a well-developed mechanism of antioxidative protection to withstand oxidative stress [52,53]. For example, O_3-exposed Mediterranean oaks activated the phenylpropanoid pathways to

counteract the accumulation of ROS and thus reduce the oxidative damage to physiological functions [54]. Moreover, other studies suggested that a leaf structure characterized by small, thick, and leathery leaves may contribute to resist O_3 stress [27,55]. Those leaves have a relatively low intercellular air space and, thus, a limited cell surface interaction with O_3 [29]. In addition, the presence of a dense layer of trichomes can often be found on the lower leaf blade, and it could increase the reaction surface with O_3, contributing to its degradation before O_3 entry into a leaf [44,56,57].

5. Conclusions

The O_3 VFI (SS_LESS, PII_ITP, and PII_FACE) increased with increasing POD_1 and did not vary with AOT40, suggesting that the new regulations for forest protection should be based on O_3 stomatal flux rather than O_3 exposure. Moreover, the new index (LIF) proposed here, which takes into account O_3 stomatal flux and leaf morphology, showed excellent results (i.e., the highest correlation coefficients with O_3 VFI both in forest sites and FACE facility) and deserves to be further explored to assess O_3 damage on forest species. To calculate the LIF index, species-specific stomatal conductance model parameters and LMA values are required. These parameters are still missing for many species, especially for shrub species such as *Viburnum lantana* [58] and *Rosa canina* [23], which often show O_3 VFI in the field. Therefore, for the practical use of LIF, further studies are needed to develop stomatal conductance models and calculate LMA for a larger array of species. Ozone is confirmed as a real and alarming threat to the health of Italian forests. Indeed, characteristic species such as *Fagus sylvatica* showed important O_3 VFI, which can translate into a decline in growth and productivity, with heavy repercussions at the ecosystem level. Conversely, conifers (*Pinus pinea* and *Picea abies*), as well as species belonging to the Mediterranean area (*Quercus* spp. and *Phillyrea latifolia*), did not show O_3 VFI, but it cannot be excluded that O_3 could affect other parameters, for example, canopy defoliation or growth reduction.

Supplementary Materials: The following are available online at https://www.mdpi.com/article/10.3390/f14050901/s1, Table S1: Stomatal conductance model parameters, where g_{max} is maximum stomatal conductance; $f_{\min}$ is minimum conductance; $f_{\text{light\_}a}$ is a parameter indicating the curvature of stomatal response curve to light; T_{max}, T_{opt}, and T_{min} are maximum, optimal, and minimum temperature for describing the variation of gs with temperature (f_{temp}); and VPD_{min} and VPD_{max} are the vapor pressure deficit for attaining minimum and maximum g_s (f_{VPD}). Table S2: Leaf Mass per Area (mean ± standard error, $n = 3$) for the species found in MOTTLES sites. Table S3: Leaf Mass per Area (mean ± standard error) for the species subjected to O_3 fumigation in FACE experiment. Table S4: Values of AOT40 and POD_1 calculated in each site for the period 2018–2022. Table S5: Species subjected to fumigation in O_3 FACE (years 2016–2020). For each species, O_3 treatment (Ambient Air, 1.5×, and 2.0×), AOT40, POD_1, and LIF are reported. Figure S1: Species-specific O_3 VFI recorded during field surveys (LESS and ITP) and FACE experiment.

Author Contributions: J.M., Y.H., B.B.M. and E.P. conceived of the study; J.M., Y.H. and B.B.M. carried out the experiment and collected the data; Y.H. and J.M. undertook the statistical analyses. Writing—original draft preparation, J.M.; writing—review and editing, Y.H., B.B.M. and E.P.; supervision, E.P. All authors have read and agreed to the published version of the manuscript.

Funding: This research was funded by MOTTLES (LIFE15 ENV/IT/000183), MODERn(NEC) (LIFE20/GIE/IT/000091), and 4ClimAir (SAC.AD002.173) projects. We also thank National Recovery and Resilience Plan (NRRP) of Italian Ministry of University and Research funded by the European Union—NextGenerationEU, Mission 4 Component 2 Investment 1.4-Avviso 3264/2021, Project Code CN_00000033, Concession Decree No. 1034 of 17 June 2022, CUP B83C22002930006, Project title "National Biodiversity Future Center-NBFC" (Spoke 5); and the Italian Integrated Environmental Research Infrastructures Systems (ITINERIS), project code IR0000032; CUP B53C22002150006.

Data Availability Statement: Data sharing is not applicable to this article as all new created data is already contained within this article.

Acknowledgments: We acknowledge all the project participants for the setting up and maintenance of the monitoring network and for contributing to the visible injury surveys in forest.

Conflicts of Interest: The authors declare no conflict of interest.

References

1. Cotrozzi, L.; Pellegrini, E.; Nali, C.; Lorenzini, G. Climate change, ozone and plant life. *Agrochimica* **2019**, *62*, 181–188.
2. Karmakar, S.P.; Das, A.B.; Gurung, C.; Ghosh, C. Effects of Ozone on Plant Health and Environment: A Mini Review. *Res. Jr. Agril. Sci.* **2022**, *13*, 612–619.
3. Xu, X.; Lin, W.; Xu, W.; Jin, J.; Wang, Y.; Zhang, G.; Zhang, X.; Ma, Z.; Dong, Y.; Ma, Q.; et al. Long-term changes of regional ozone in China: Implications for human health and ecosystem impacts. *Elem. Sci. Anthr.* **2020**, *8*, 13. [CrossRef]
4. Sicard, P. Ground-level ozone over time: An observation-based global overview. *Curr. Opin. Environ. Sci. Health* **2021**, *19*, 100226. [CrossRef]
5. Meleux, F.; Solmon, F.; Giorgi, F. Increase in summer European ozone amounts due to climate change. *Atmos. Environ.* **2007**, *41*, 7577–7587. [CrossRef]
6. Young, P.J.; Archibald, A.T.; Bowman, K.W.; Lamarque, J.-F.; Naik, V.; Stevenson, D.S.; Tilmes, S.; Voulgarakis, A.; Wild, O.; Bergmann, D.; et al. Pre-industrial to end 21st century projections of tropospheric ozone from the Atmospheric Chemistry and Climate Model Intercomparison Project (ACCMIP). *Atmos. Chem. Phys.* **2013**, *13*, 2063–2090. [CrossRef]
7. Sicard, P.; Anav, A.; De Marco, A.; Paoletti, E. Projected global ground-level ozone impacts on vegetation under different emission and climate scenarios. *Atmos. Chem. Phys.* **2017**, *17*, 12177–12196. [CrossRef]
8. Pay, M.T.; Gangoiti, G.; Guevara, M.; Napelenok, S.; Querol, X.; Jorba, O.; Pérez García-Pando, C. Ozone source apportionment during peak summer events over southwestern Europe. *Atmos. Chem. Phys.* **2019**, *19*, 5467–5494. [CrossRef]
9. Grulke, N.E.; Heath, R.L. Ozone effects on plants in natural ecosystems. *Plant Biol.* **2020**, *22*, 12–37. [CrossRef]
10. Emberson, L. Effects of ozone on agriculture, forests and grasslands. *Philos. Trans. R. Soc. A* **2020**, *378*, 20190327. [CrossRef]
11. Harmens, H.; Mills, G. *Ozone pollution: Impacts on Carbon Sequestration in Europe*; NERC/Centre for Ecology & Hydrology: Lancaster, UK, 2012.
12. Agathokleous, E.; Feng, Z.; Oksanen, E.; Sicard, P.; Wang, Q.; Saitanis, C.J.; Araminiene, V.; Blande, J.D.; Hayes, F.; Calatayud, V.; et al. Ozone affects plant, insect, and soil microbial communities: A threat to terrestrial ecosystems and biodiversity. *Sci. Adv.* **2020**, *6*, eabc1176. [CrossRef]
13. Sharma, P.; Jha, A.B.; Dubey, R.S.; Pessarakli, M. Reactive oxygen species, oxidative damage, and antioxidative defense mechanism in plants under stressful conditions. *J. Bot.* **2012**, *2012*, 217037. [CrossRef]
14. Hoshika, Y.; Fares, S.; Savi, F.; Gruening, C.; Goded, I.; De Marco, A.; Sicard, P.; Paoletti, E. Stomatal conductance models for ozone risk assessment at canopy level in two Mediterranean evergreen forests. *Agric. For. Meteorol.* **2017**, *234*, 212–221. [CrossRef]
15. Hoshika, Y.; Carrari, E.; Mariotti, B.; Martini, S.; De Marco, A.; Sicard, P.; Paoletti, E. Flux-Based Ozone Risk Assessment for a Plant Injury Index (PII) in Three European Cool-Temperate Deciduous Tree Species. *Forests* **2020**, *11*, 82. [CrossRef]
16. Proietti, C.; Anav, A.; De Marco, A.; Sicard, P.; Vitale, M. A multi-sites analysis on the ozone effects on Gross Primary Production of European forests. *Sci. Total Environ.* **2016**, *556*, 1–11. [CrossRef]
17. Leisner, C.P.; Ainsworth, E.A. Quantifying the effects of ozone on plant reproductive growth and development. *Glob. Change Biol.* **2012**, *18*, 606–616. [CrossRef]
18. Mills, G.; Pleijel, H.; Malley, C.S.; Sinha, B.; Cooper, O.R.; Schultz, M.G.; Neufeld, H.S.; Simpson, D.; Sharps, S.; Feng, Z.; et al. Tropospheric Ozone Assessment Report: Present–day tropospheric ozone distribution and trends relevant to vegetation. *Elem. Sci. Anth.* **2018**, *6*, 47. [CrossRef]
19. Calatayud, V.; Cerveró, J.; Sanz, M.J. Foliar, Physiological and growth responses of four maple species exposed to ozone. *Water Air Soil Pollut.* **2007**, *185*, 239–254. [CrossRef]
20. Li, P.; Calatayud, V.; Gao, F.; Uddling, J.; Feng, Z. Differences in ozone sensitivity among woody species are related to leaf morphology and antioxidant levels. *Tree Physiol.* **2016**, *36*, 1105–1116. [CrossRef] [PubMed]
21. Moura, B.B.; Alves, E.S.; Marabesi, M.A.; Ribeiro de Souza, S.; Schaub, M.; Vollenweider, P. Ozone affects leaf physiology and causes injury to foliage of native tree species from the tropical Atlantic Forest of southern Brazil. *Sci. Total Environ.* **2018**, *610–611*, 912–925. [CrossRef] [PubMed]
22. Sicard, P.; Hoshika, Y.; Carrari, E.; De Marco, A.; Paoletti, E. Testing visible ozone injury within a Light Exposed Sampling Site as a proxy for ozone risk assessment for European forests. *J. For. Res.* **2021**, *32*, 1351–1359. [CrossRef]
23. Moura, B.B.; Carrari, E.; Dalstein-Richier, L.; Sicard, P.; Leca, S.; Badea, O.; Pitar, D.; Shashikumar, A.; Cirani, M.L.; Paoletti, E.; et al. Bridging experimental and monitoring research for visible foliar injury as bio-indicator of ozone impacts on forests. *Ecosyst. Health Sustain.* **2022**, *8*, 2144466. [CrossRef]
24. European Council Directive 2008/50/EC of the European Parliament and of the council of 21st May 2008 on ambient air quality and cleaner air for Europe. *Off. J. Eur. Union* **2008**, *152*, 1–44.
25. Paoletti, E.; Alivernini, A.; Anav, A.; Badea, O.; Carrari, E.; Chivulescu, S.; Conte, A.; Ciriani, M.L.; Dalstein-Richer, L.; De Marco, A.; et al. Toward stomatal–flux based forest protection against ozone: The MOTTLES approach. *Sci. Total Environ.* **2019**, *691*, 516–527. [CrossRef]
26. De Marco, A.; Proietti, C.; Anav, A.; Ciancarella, L.; D'Elia, I.; Fares, S.; Fornasier, M.F.; Fusaro, L.; Gualtieri, M.; Manes, F.; et al. Impacts of air pollution on human and ecosystem health, and implications for the National Emission Ceilings Directive: Insights from Italy. *Environ. Int.* **2019**, *125*, 320–333. [CrossRef]

27. Bussotti, F. Functional leaf traits, plant communities and acclimation processes in relation to oxidative stress in trees: A critical overview. *Glob. Change Biol.* **2008**, *14*, 2727–2739. [CrossRef]
28. Feng, Z.; Büker, P.; Pleijel, H.; Emberson, L.; Karlsson, P.E.; Uddling, J. A unifying explanation for variation in ozone sensitivity among woody plants. *Glob. Change Biol.* **2018**, *24*, 78–84. [CrossRef]
29. Bennett, J.P.; Rassat, P.; Berrang, P.; Karnosky, D.F. Relationships between leaf anatomy and ozone sensitivity of *Fraxinus pennsylvanica marsh*. and *Prunus serotina* Ehrh. *Environ. Exp. Bot.* **1992**, *32*, 33–41. [CrossRef]
30. Wieser, G.; Hecke, K.; Tausz, M.; Matyssek, R. Foliage type specific susceptibility to ozone in *Picea abies*, *Pinus cembra* and *Larix decidua* at treeline: A synthesis. *Environ. Exp. Bot.* **2013**, *90*, 4–11. [CrossRef]
31. Paoletti, E.; Materassi, A.; Fasano, G.; Hoshika, Y.; Carriero, G.; Silaghi, D.; Badea, O. A new-generation 3D ozone FACE (free air controlled exposure). *Sci. Total Environ.* **2017**, *575*, 1407–1414. [CrossRef]
32. CLRTAP, 2017. Mapping Critical Levels for Vegetation, Chapter III of Manual on Methodologies and Criteria for Modelling and Mapping Critical Loads and Levels and Air Pollution Effects, Risks and Trends. UNECE Convention on Long-Range Transboundary Air Pollution. Available online: www.icpmapping.org (accessed on 1 July 2022).
33. Paoletti, E.; Sicard, P.; Hoshika, Y.; Fares, S.; Badea, O.; Pitar, D.; Popa, I.; Anav, A.; Barbara, B.B.; De Marco, A. Towards long-term sustainability of stomatal ozone flux monitoring at forest sites. *Sustain. Horiz.* **2022**, *2*, 100018. [CrossRef]
34. Jarvis, P.G. Interpretation of variations in leaf water potential and stomatal conductance found in canopies in field. *Philos. Trans. R. Soc. Lond. B* **1976**, *273*, 593–610.
35. Anav, A.; De Marco, A.; Proietti, C.; Alessandri, A.; Dell'Aquila, A.; Cionni, I.; Friedlingstein, P.; Khvorostyanov, D.; Menut, L.; Paoletti, E.; et al. Comparing concentration-based (AOT40) and stomatal uptake (PODY) metrics for ozone risk assessment to European forests. *Glob. Change Biol.* **2016**, *22*, 1608–1627. [CrossRef] [PubMed]
36. Hoshika, Y.; Osada, Y.; De Marco, A.; Penuelas, J.; Paoletti, E. Global diurnal and nocturnal parameters of stomatal conductance in woody plants and major crops. *Glob. Ecol. Biogeogr.* **2018**, *27*, 257–275. [CrossRef]
37. Easlon, H.M.; Bloom, A.J. Easy Leaf Area: Automated digital image analysis for rapid and accurate measurement of leaf area. *Appl. Plant Sci.* **2014**, *2*, 1400033. [CrossRef]
38. Schaub, M.; Calatayud, V.; Ferretti, M.; Brunialti, G.; Lövblad, G.; Krause, G.; Sanz, M.J. Part VIII: Monitoring of Ozone Injury. In *UNECE ICP Forests Programme Coordinating Centre (Ed) Manual on Methods and Criteria for Harmonized Sampling, Assessment, Monitoring and Analysis of the Effects of Air Pollution on Forests*; Thünen Institute of Forest Ecosystems: Eberswalde, Germany, 2016; p. 14.
39. Paoletti, E.; Ferrara, A.M.; Calatayud, V.; Cerveró, J.; Giannetti, F.; Sanz, M.J.; Manning, W.J. Deciduous shrubs for ozone bioindication: Hibiscus syriacus as an example. *Environ. Pollut.* **2009**, *157*, 865–870. [CrossRef]
40. Gerosa, G.; Marzuoli, R.; Bussotti, F.; Pancrazi, M.; Ballarin-Denti, A. Ozone sensitivity of *Fagus sylvatica* and *Fraxinus excelsior* young trees in relation to leaf structure and foliar ozone uptake. *Environ. Pollut.* **2003**, *125*, 91–98. [CrossRef]
41. Vollenweider, P.; Günthardt-Goerg, M.S.; Menard, T.; Baumgarten, M.; Matyssek, R.; Schaub, M. Macro- and microscopic leaf injury triggered by ozone stress in beech foliage (*Fagus sylvatica* L). *Ann. For. Sci.* **2019**, *76*, 71. [CrossRef]
42. VanderHeyden, D.; Skelly, J.; Innes, J.; Hug, C.; Zhang, J.; Landolt, W.; Bleuler, P. Ozone exposure thresholds and foliar injury on forest plants in Switzerland. *Environ. Pollut.* **2001**, *111*, 321–331. [CrossRef]
43. Paoletti, E. Ozone impacts on Mediterranean forests: A review. *Environ. Pollut.* **2006**, *144*, 463–474. [CrossRef]
44. Calatayud, V.; Cerveró, J.; Calvo, E.; García-Breijo, F.J.; Reig-Armiñana, J.; Sanz, M.J. Responses of evergreen and deciduous Quercus species to enhanced ozone levels. *Environ. Pollut.* **2011**, *159*, 55–63. [CrossRef] [PubMed]
45. Nunn, A.J.; Kozovits, A.R.; Reiter, I.M.; Heerdt, C.; Leuchner, M.; Lutz, C.; Liu, X.; Low, M.; Winkler, J.B. Comparison of ozone uptake and sensitivity between a phytotron study with young beech and a field experiment with adult beech (*Fagus sylvatica*). *Environ. Pollut.* **2005**, *137*, 494–506. [CrossRef] [PubMed]
46. Kolb, T.E.; Matyssek, R. Limitations and perspectives about scaling ozone impacts in trees. *Environ. Pollut.* **2001**, *115*, 373–393. [CrossRef] [PubMed]
47. Ryan, M.G.; Phillips, N.; Bond, B.J. The hydraulic limitation hypothesis revisited. *Plant Cell Environ.* **2006**, *29*, 367–381. [CrossRef] [PubMed]
48. Hoshika, Y.; Cotrozzi, L.; Marchica, A.; Carrari, E.; Lorenzini, G.; Nali, C.; Paoletti, E.; Pellegrini, E. Season-long exposure of bilberry plants to realistic and future ozone pollution improves the nutraceutical quality of fruits. *Sci. Total Environ.* **2022**, *822*, 153577. [CrossRef]
49. Sicard, P.; De Marco, A.; Carrari, E.; Dalstein-Richier, L.; Hoshika, Y.; Badea, O.; Pitar, D.; Fares, S.; Conte, A.; Popa, I.; et al. Epidemiological derivation of flux-based critical levels for visible ozone injury in European forests. *J. For. Res.* **2020**, *31*, 1509–1519. [CrossRef]
50. Hoshika, Y.; Fares, S.; Pellegrini, E.; Conte, A.; Paoletti, E. Water use strategy affects avoidance of ozone stress by stomatal closure in Mediterranean trees–A modelling analysis. *Plant Cell Environ.* **2020**, *43*, 611–623. [CrossRef]
51. Matyssek, R.; Bytnerowicz, A.; Karlsson, P.E.; Paoletti, E.; Sanz, M.; Schaub, M.; Wieser, G. Promoting the O_3 flux concept for European forest trees. *Environ. Pollut.* **2007**, *146*, 587–607. [CrossRef]
52. Munné-Bosch, S.; Peñuelas, J. Drought-induced oxidative stress in strawberry tree (*Arbutus unedo* L.) growing in Mediterranean field conditions. *Plant Sci.* **2004**, *166*, 1105–1110. [CrossRef]

53. Fernández-Marín, B.; Hernández, A.; Garcia-Plazaola, J.I.; Esteban, R.; Míguez, F.; Artetxe, U.; Gómez-Sagasti, M.T. Photoprotective strategies of Mediterranean plants in relation to morphological traits and natural environmental pressure: A meta-analytical approach. *Front. Plant Sci.* **2017**, *8*, 1051. [CrossRef]
54. Pellegrini, E.; Hoshika, Y.; Dusart, N.; Cotrozzi, L.; Gérard, J.; Nali, C.; Vaultier, M.-N.; Jolivet, Y.; Lorenzini, G.; Paoletti, E. Antioxidative responses of three oak species under ozone and water stress conditions. *Sci. Total Environ.* **2019**, *647*, 390–399. [CrossRef] [PubMed]
55. Bussotti, F.; Desotgiu, R.; Cascio, C.; Strasser, R.J.; Gerosa, G.; Marzuoli, R. Photosynthesis responses to ozone in young trees of three species with different sensitivities, in a 2-year open-top chamber experiment (Curno, Italy). *Physiol. Plant.* **2007**, *130*, 122–135. [CrossRef]
56. Li, S.; Tosens, T.; Harley, P.C.; Jiang, Y.; Kanagendran, A.; Grosberg, M.; Jaamets, K.; Niinemets, Ü. Glandular trichomes as a barrier against atmospheric oxidative stress: Relationships with ozone uptake, leaf damage, and emission of LOX products across a diverse set of species. *Plant Cell Environ.* **2018**, *41*, 1263–1277. [CrossRef]
57. Oksanen, E. Trichomes form an important first line of defence against adverse environment—New evidence for ozone stress mitigation. *Plant Cell Environ.* **2018**, *41*, 1497–1499. [CrossRef]
58. Gottardini, E.; Cristofori, A.; Cristofolini, F.; Nali, C.; Pellegrini, E.; Bussotti, F.; Ferretti, M. Chlorophyll-related indicators are linked to visible ozone symptoms: Evidence from a field study on native *Viburnum lantana* L. plants in northern Italy. *Ecol. Indic.* **2014**, *39*, 65–74. [CrossRef]